THE JOURNAL OF BIOLOGICAL CHEMISTRY
Vol. 278, No. 7, Issue of February 14, pp. 4572–4581, 2003
Printed in U.S.A.

Differences on the Inhibitory Specificities of H-Ras, K-Ras, and N-Ras (N17) Dominant Negative Mutants Are Related to Their Membrane Microlocalization*

Received for publication, September 24, 2002, and in revised form, November 19, 2002
Published, JBC Papers in Press, November 27, 2002, DOI 10.1074/jbc.M209807200

David Matallanas‡, Imanol Arozarena‡§¶, María T. Berciano‖, David S. Aaronson§, Angel Pellicer‡‡§§, Miguel Lafarga‖, and Piero Crespo‡§¶¶**

From the §Departamentos de Biología Molecular and ‖Anatomía y Biología Celular, Universidad de Cantabria, Santander 39011, Spain, the ‡‡Department of Pathology and Kaplan Comprehensive Cancer Center, New York University School of Medicine, New York, New York 10016, and the ‡Instituto de Investigaciones Biomédicas, Consejo Superior de Investigaciones Centíficas, Arturo Duperier 4, Madrid 28029, Spain

Ras GTPases include the isoforms H-Ras, K-Ras, and N-Ras. Despite their great biochemical and biological similarities, evidence is mounting suggesting that Ras proteins may not be functionally redundant. A widespread strategy for studying small GTPases is the utilization of dominant inhibitory mutants that specifically block the activation of their respective wild-type proteins. As such, H-Ras N17 has proved to be extremely valuable as a tool to probe Ras functions. However, a comparative study on the inhibitory specificities of H-, K-, and N-Ras N17 mutants has not been approached thus far. Herein, we demonstrate that H-, K-, and N-Ras N17 mutants exhibit markedly distinct inhibitory effects toward H-, K-, and N-Ras. H-Ras N17 can effectively inhibit the activation of all three isoforms. K-Ras N17 completely blocks the activation of K-Ras and is only slightly inhibitory on H-Ras. N-Ras N17 can mainly inhibit N-Ras activation. In light of the recent data on the compartmentalization of H-Ras and K-Ras in the plasma membrane, here we present for the first time a description of N-Ras cellular microlocalization. Overall, our results on Ras N17 mutants specificities exhibit a marked correlation with the localization of the Ras isoforms to distinct membrane microdomains.

Ras GTPases are essential mediators in signaling pathways that convey extracellular signals from surface receptors to the interior of the cell, functioning as molecular switches in processes governing cell proliferation, survival, and differentiation (1, 2). The three mammalian *ras* genes encode for four proteins: H-Ras, K-Ras4A, K-Ras4B, and N-Ras, of 189 amino acids (188 in K-Ras4B) and 21 kDa. These proteins are identical over the N-terminal 85 residues, and their identity is up to 90% within the following 80 residues. The main divergence among Ras isoforms is restricted to the 24 C-terminal amino acids, in which less than 15% of the residues are identical between any pair of proteins, with the sole exception of cysteine 186. For this reason, this segment has been termed the heterogeneous or hypervariable region (3). This region contains an essential signal for localizing Ras to the inner surface of the plasma membrane, the CAA*X* box (C = cysteine, A = alyphatic amino acid, and *X* = serine/methionine), located at the extreme C terminus. The CAA*X* box suffers a post-translational modification that makes it more hydrophobic. The cysteine is farnesylated, the AA*X* sequence is proteolyzed, and the newly C-terminal cysteine is carboxymethylated (4). A second signal is required for efficiently positioning Ras in the membrane. This is accomplished by palmitoylation of cysteine 181 in N-Ras and cysteines 181 and 184 in H-Ras. In the case of K-Ras4B the second signal consist of a polybasic motif of six lysines (175–180) that is believed to interact electrostatically with the negatively charged membrane (5–7).

In mammalians, the three *ras* genes are ubiquitously expressed, even though the expression pattern for each gene is quantitatively different depending on the organ (8, 9). Variations in the expression pattern also exist throughout embryonic development (8, 10) and during differentiation processes (2). But despite these differences, no instance has been reported in which the expression of any one of the three *ras* genes is completely absent. This has lead to the notion that, regardless of their great similarities, the functions of the three Ras proteins may not be completely redundant. In this line, during these past years a considerable amount of data has been accumulated that speaks in favor of the three Ras proteins having differential functions. As such, different *ras* genes are activated in different human tumors (11, 12). Likewise, the three *ras* genes have different transforming potential depending on the cell line (13), suggestive of cell-specific activities. Ras proteins exhibit distinct sensitivities to inhibition by GAPs (14) and to activation by guanine-nucleotide exchange factors (GEFs)[1] (15, 16). Also, regarding effector interactions, Ras isoforms vary in their ability to activate Raf, phosphoinositide 3-kinase, and Rac-1 (17–19). But perhaps the most compelling evidence advocating for the three Ras proteins having distinct functions

* This work was supported by Grant PM 98-0131 from the Spanish Ministry of Education and Grant 01-087 from the Association for International Cancer Research. The costs of publication of this article were defrayed in part by the payment of page charges. This article must therefore be hereby marked "*advertisement*" in accordance with 18 U.S.C. Section 1734 solely to indicate this fact.

¶ Predoctoral fellow of the Spanish Ministry of Education.

** Present address: Mount Sinai School of Medicine, One Gustave L. Levi Place, New York, NY 10029-6574.

§§ Supported by National Institutes of Health Grant CA-36327.

¶¶To whom correspondence should be addressed: Instituto de Investigaciones Biomédicas, Consejo Superior de Investigaciones Centíficas, Arturo Duperier 4, Madrid, 28029, Spain. Tel.: 34-91-5854886; Fax: 34-91-5854587; E-mail: pcrespo@iib.uam.es.

[1] The abbreviations used are: GEF, guanine-nucleotide exchange factor; HA, hemagglutinin; MDCK, Madin-Darby canine kidney; MEF, mouse embryo fibroblast; EGF, epidermal growth factor; PDGF, platelet-derived growth factor; LPA, lysophosphatidic acid; ERK, extracellular signal-regulated kinase; MBP, myelin basic protein; PBS, phosphate-buffered saline; MEK, mitogen-activated protein kinase/extracellular signal-regulated kinase kinase; GST, glutathione *S*-transferase; GFP, green fluorescent protein.

has been provided by gene targeting experiments. It has been found that N-*ras* knock-out mice develop and reproduce normally (20). H-*ras* knock-out animals are also normal (21). Strikingly, H- and N-*ras* double knock-outs also exhibit no detectable abnormalities (22). On the other hand, K-*ras*-deficient mice die during embryonic development (23, 24), suggesting that K-Ras possesses functions not shared by H- or N-Ras.

Recently, a considerable body of evidence has been accumulated suggesting that the aforementioned biochemical and biological differences among Ras isoforms could be due, in part, to variations in plasma membrane microlocalization (25). In this line, it has been shown that H-Ras is equally localized in caveolae, lipid rafts, and disordered membrane. By contrast, K-Ras is preferentially located in disordered, nonraft plasma membrane (26), although some may be present in caveolae depending on the cell type (27). Likewise, N-Ras localizes to caveolin-positive and caveolin-negative domains (27), but its detailed microlocalization has not been examined so far. Recent reports also demonstrate that all of the information required for membrane localization is contained in the hypervariable regions of the Ras isoforms (28, 29) that also dictate how Ras proteins traffic to their final locations. Whereas H- and N-Ras traffic to the plasma membrane along the secretory pathway through the Golgi complex, K-Ras4B is directly routed from the endoplasmic reticulum to the membrane by still unknown mechanisms (30, 31).

Multiple strategies have been utilized thus far to unveil the functions of Ras proteins in cells. Among these, the use of dominant inhibitory mutants is now widely established (32). Ever since its identification (33, 34) the Ras mutant with a substitution of serine 17 by aspargine (Ras N17) and its homologues have been invaluable tools in the extensive progress that has been made in our understanding of the roles of Ras-related GTPases in general and of Ras in particular. It is now accepted that Ras N17 mutants work *in vivo* by competing with wild-type Ras for binding to exchange factors. Because N17 mutants have a higher affinity for exchange factors than does normal Ras, and they cannot interact with downstream effectors, this results in the formation of unproductive complexes, thereby preventing the activation of endogenous Ras (32). As such, it could be concluded that rather than inhibiting Ras itself, N17 mutants inhibit the function of exchange factors. Consistently, because most Ras exchange factors can activate H-, K-, and N- Ras, at least *in vitro* (35), the expression of one Ras N17 mutant could be predicted to block the activation of the other two Ras isoforms. This conceptual pitfall may have precluded a more extensive use of the N17 mutants for the study of the differential functions of the three Ras isoforms. However, a comparative study on the specificities of H-, K-, and N-Ras dominant inhibitory mutants has not been approached experimentally so far.

Herein, we have undertaken that challenge. We demonstrate that H-, K-, and N-Ras N17 mutants exhibit markedly distinct specificities on their inhibitory functions. H-Ras N17 can inhibit the activation of all three isoforms. K-Ras N17 completely inhibits the activation of K-Ras and, slightly, that of H-Ras. Likewise, N-Ras N17 can chiefly inhibit N-Ras activation. These results can be explained in light of the recent data on the compartmentalization of Ras proteins. In this respect, we present for the first time a detailed description of N-Ras cellular microlocalization.

MATERIALS AND METHODS

Constructs—Plasmids encoding for CAL-DAG I and III were provided by M. Matsuda; Ras-GRP (CAL-DAG II) was provided by J.C. Stone; Ras-GRF2 was provided by M.F. Moran. K-Ras4B N17, N-Ras N17, and H-Ras ΔCAA*X* (lacking Cys^{186}) and N-Ras S186C were generated by PCR-directed mutagenesis and verified by sequencing. Sequences of the oligonucleotides utilized are available upon request. The inserts were cloned in pCEFL, a modified pCDNA3 in which the cytomegalovirus promoter was substituted for the EF-1α promoter, containing an N-terminal hemagglutinin (HA), a FLAG or an AU5 tag, or a Src myristoylation signal, as indicated. H-Ras, N-Ras, and N-Ras C-terminal 26 amino acids (hypervariable region) were cloned in pEGFP-C1.

Cell Culture—COS-7, NIH3T3, and MDCK cells were regularly grown in Dulbecco's modified Eagle's medium supplemented with 10% fetal calf serum (new born, for NIH3T3). COS-7 subconfluent cells were transfected by the DEAE-dextran technique (36). MEFs were regularly grown in Dulbecco's modified Eagle's medium supplemented with 10% fetal calf serum, L-glutamine 2 mM, 0.1 mM minimum essential medium nonessential amino acids, β-mercaptoethanol 55 μM. MEFs, NIH3T3, and MDCK cells were transfected with LipofectAMINE (Invitrogen) following the manufacturer's instructions. EGF and PDGF were from Upstate Biotechnology, Inc. LPA was from Sigma.

Kinase Assays—ERK2 kinase activities were determined as previously described (37), in anti-HA immunoprecipitates using myelin basic protein (MBP) as substrate (Sigma).

Immunoblotting—Total lysates and immunoprecipitates were fractionated in SDS-PAGE gels and transferred onto nitrocellulose filters as described (38). Immunocomplexes were visualized by ECL detection (Amersham Biosciences) using horseradish peroxidase-conjugated secondary antibodies (Cappel). Mouse monoclonal antibodies anti-AU5 and anti-HA antibodies were from Babco. Mouse monoclonal anti-FLAG was from Invitrogen. Mouse monoclonal antibodies anti-H-Ras, -K-Ras, -N-Ras, and -caveolin were from Santa Cruz Laboratories. Mouse monoclonal anti-Pan-Ras was from Calbiochem.

Ras GTP Loading—Ras GTP loading was performed basically as described (39). Briefly, HA-Ras-transfected cells were lysed in HEM buffer (25 mM HEPES, pH 7.3, 10 mM $MgCl_2$, 150 mM NaCl, 0.5 mM EGTA, 20 mM β-glycerophosphate, 0.5% Nonidet-P40, 4% glycerol, 2 mM sodium orthovanadate, 1 mM phenylmethylsulfonyl fluoride, 25 μg/ml leupeptin, and 25 μg/ml aprotinin. HA-Ras was affinity sequestered with bacterially synthesized GST-Raf Ras-binding domain (amino acids 1–149). Immunoblots were performed as described above using anti-HA antibody and quantitated by densitometry, using the program NIH Image 1.60. Ras-GTP levels were related to total Ras protein levels as determined by anti-HA immunoblotting in the corresponding total lysates.

Subcellular Fractionation—Subcellular fractionation was performed in 20 mM HEPES pH 7.4 buffer, basically as described (37).

Sucrose Gradients—The cells were collected and resuspended in 25 mM Tris, pH 7.4, 150 mM NaCl, 5 mM EDTA, and 0.25% Triton X-100, rocking at 4 °C for 1 h. The lysates were set to a sucrose concentration of 41%. Layers of 8.5 ml of 35% sucrose (in 10 mM Tris, pH 7.4) and of 2.5 ml 16% sucrose were sequentially overlaid and centrifuged in a Beckman SW41 rotor for 18 h at 35000 rpm. Eleven or twelve 1-ml fractions were collected, precipitated in 6.5% trichloroacetic acid, resuspended in loading buffer, and fractionated in 12% SDS-PAGE gels.

Immunoelectron Microscopy—MDCK cells transfected with vector, GFP-H-Ras, GFP-N-Ras, and GFP-N-Ras-hypervariable region were fixed with 4% paraformaldehyde in 0.1 M phosphate buffer for 1 h at room temperature. The cells were scraped, transferred to an Eppendorf tube, and centrifuged for 10 min. The pellets were washed with 0.1 M phosphate buffer, dehydrated in increasing concentrations of methanol at −20 °C, embedded in Lowicryl K4M at −20 °C, and polymerized with ultraviolet irradiation. Ultrathin sections were mounted on nickel grids and sequentially incubated with 0.1 M glycine in PBS for 15 min, with 5% bovine serum albumin in PBS for 1 h, and finally with the monoclonal anti-GFP antibodies (clones 7.1 and 13.1; Roche Molecular Biochemicals) for 1 h (diluted 1:100 in PBS, 1% bovine serum albumin, 0.1 M glycine). After washing, the sections were incubated with goat anti-mouse IgG coupled to 10-nm gold particles (BioCell; diluted 1:50 in PBS, 1% bovine serum albumin). After immunogold labeling, the ultrathin sections were stained with uranyl acetate and lead citrate and examined with a Philips EM208 electron microscope operated at 60 kV. As controls, ultrathin sections were treated as described above but omitting the primary antibody.

RESULTS

To avoid misinterpretations, an initial requisite in this project was to verify that the Ras isoforms under study were expressed in those cell lines to be utilized. Using antibodies that specifically recognize H-Ras, K-Ras, and N-Ras, we ascertained that these proteins were detectable in lysates from

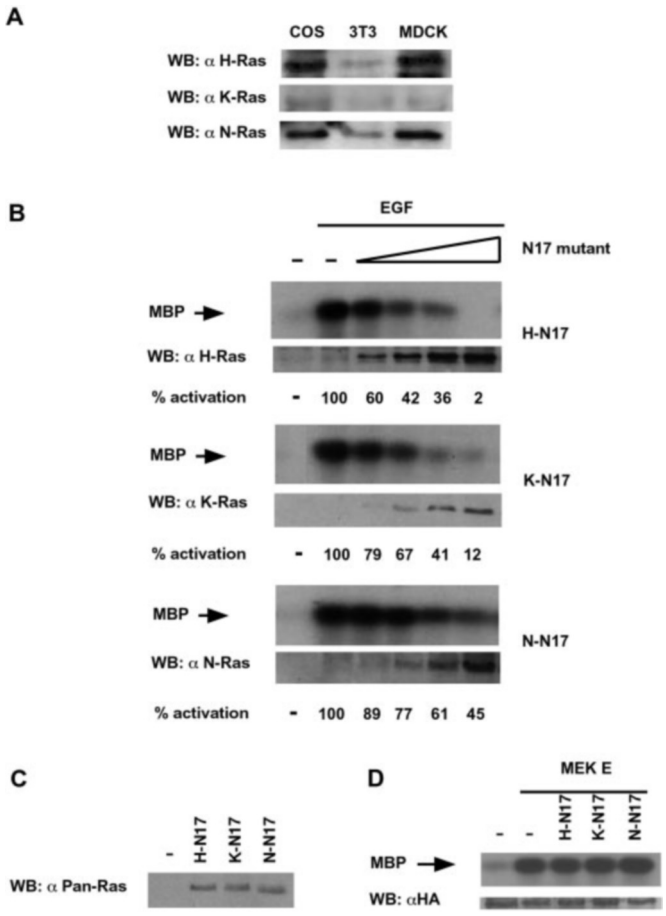

FIG. 1. *A*, endogenous levels of H-Ras, K-Ras, and N-Ras in COS-7, NIH3T3, and MDCK cells. Cells from confluent 100-mm plates were collected in PBS, and pellets were lysed in 250 μl of lysis buffer. The proteins were fractionated by PAGE, and Western blots (*WB*) were performed using antibodies that specifically recognize the three Ras isoforms. *B*, concentration-dependent inhibition of the activation of ERK2 by Ras dominant inhibitory mutants. Kinase assays were performed using MBP as substrate, in anti-HA immunoprecipitates from COS-7 cells co-transfected with HA-ERK2 (1 μg) and with vector (−) or with increasing concentrations (50, 100, 200, and 250 ng) of constructs encoding H-N17, K-N17, and N-N17 as indicated, and stimulated with EGF (100 ng/ml) for 5 min after 12 h of serum starvation. *Lower panels*, protein levels of H-N17, K-N17, and N-N17 as determined by immunoblotting using isoform-specific antibodies. The panels show the average activation relative to EGF-treated cells from three independent experiments. *C*, expression levels of H-N17, K-N17, and N-N17 in total cellular lysates, resulting from transfection of 250 ng of their respective coding constructs, as determined by anti-Pan-Ras immunoblotting. *D*, effects of Ras dominant inhibitory mutants on the activation of ERK2 induced by MEK1. Kinase assays were performed in anti-HA immunoprecipitates from COS-7 cells transfected with HA-ERK2 (1 μg) in addition to MEK1 EE (1 μg) and plasmids encoding for H-N17, K-N17, and N-N17 (250 ng). *Lower panel*, protein levels of HA-ERK2 as determined by immunoblotting using an HA-specific antibody.

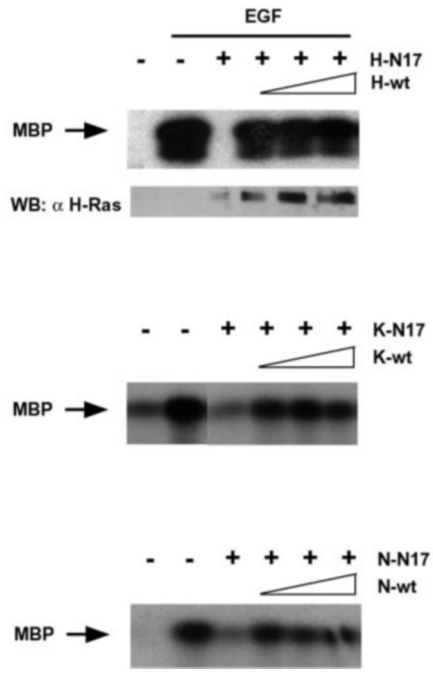

FIG. 2. **Inhibition by H-, K-, and N-Ras N17 mutants is rescued by the overexpression of their respective wild-type proteins.** COS-7 cells were co-transfected with AU5-ERK2 (1 μg), with vector (−) or with 250 ng of constructs for H-N17, K-N17, and N-N17 (+) as indicated in the different panels, in addition to increasing concentrations (500 ng, 750 ng, and 1 μg) of plasmids encoding H-, K-, or N-Ras wild types (*wt*). Upon stimulation with EGF (100 ng/ml) for 5 min, after 12 h of serum starvation, the kinase assays were performed in anti-AU5 immunoprecipitates, using MBP as substrate, as described under "Materials and Methods." *Lower panel*, protein levels of H-Ras as determined by immunoblotting using an H-Ras-specific antibody. *WB*, Western blot.

COS-7, NIH3T3, and MDCK cells (Fig. 1*A*), thereby validating these three cell lines for further experimentation. As a first approach to investigate the specificity of H-, K(4B)-, and N-Ras N17 mutants (referred to as H-N17, K-N17, and N-N17 hereafter), we compared the inhibitory potential that each of the Ras dominant interfering mutants displayed against a Ras-activating stimulus such as EGF (40). As a readout, we utilized the activation of ERK2, whose activation by EGF in COS-7 cells has been previously shown to be potently inhibited by the original H-N17 (41). For this purpose, COS-7 cells were transiently transfected with HA-ERK2 and with increasing concentrations of the three inhibitory mutants. Upon stimulation with EGF it was found that H-, K-, and N-N17 were capable of diminishing EGF-induced activation of ERK2, although to different extents. At the maximum expression levels, H-N17 caused a total repression on ERK2 activation, K-N17 inhibited EGF-induced ERK2 activity by 88%, and N-N17 exhibited the least inhibitory effect, only reaching a 55% inhibition (Fig. 1*B*). We also monitored the protein levels of the three N17 mutants using antibodies specific for H-, K-, and N-Ras, verifying that, in all three cases, the augmentation in their inhibitory effects correlated with an increase in their protein levels (Fig. 1*B*, *bottom panels*). Because intrinsic variations in the affinity of the Ras isoform-specific antibodies precluded a comparison of the isoforms protein levels, we also utilized a pan-Ras antibody that recognizes equally the three Ras isoforms to ascertain that variations in the inhibitory potential of the N17 mutants were not due to differences in their expression. As shown in Fig. 1*C*, the protein levels of the three N17 mutants, resulting from the transfection of 250 ng of their coding constructs, were similar. To make sure that the inhibitory effects of the Ras N17 mutants were not due to some unspecific, Ras-independent process, we co-transfected a constitutively active mutant of MEK1 (MEKE), known to act downstream from Ras (36), with H-N17, K-N17 and N-N17 mutants. It was found that the activation of ERK2 by MEKE was completely unaffected by the Ras inhibitory mutants (Fig. 1*D*), thus verifying that the inhibitory effects of H-, K-, and N-Ras dominant interfering mutants were Ras-mediated.

It is well known that the inhibitory effects of Ras N17 can be overcome by the increased expression of wild-type Ras (34, 42). Therefore, we tested whether the inhibition of EGF-induced activation of ERK2 by H-, K-, and N-Ras inhibitory mutants could be rescued by an overexpression of their respective wild-type proteins. As such, the cells were transfected with H-N17,

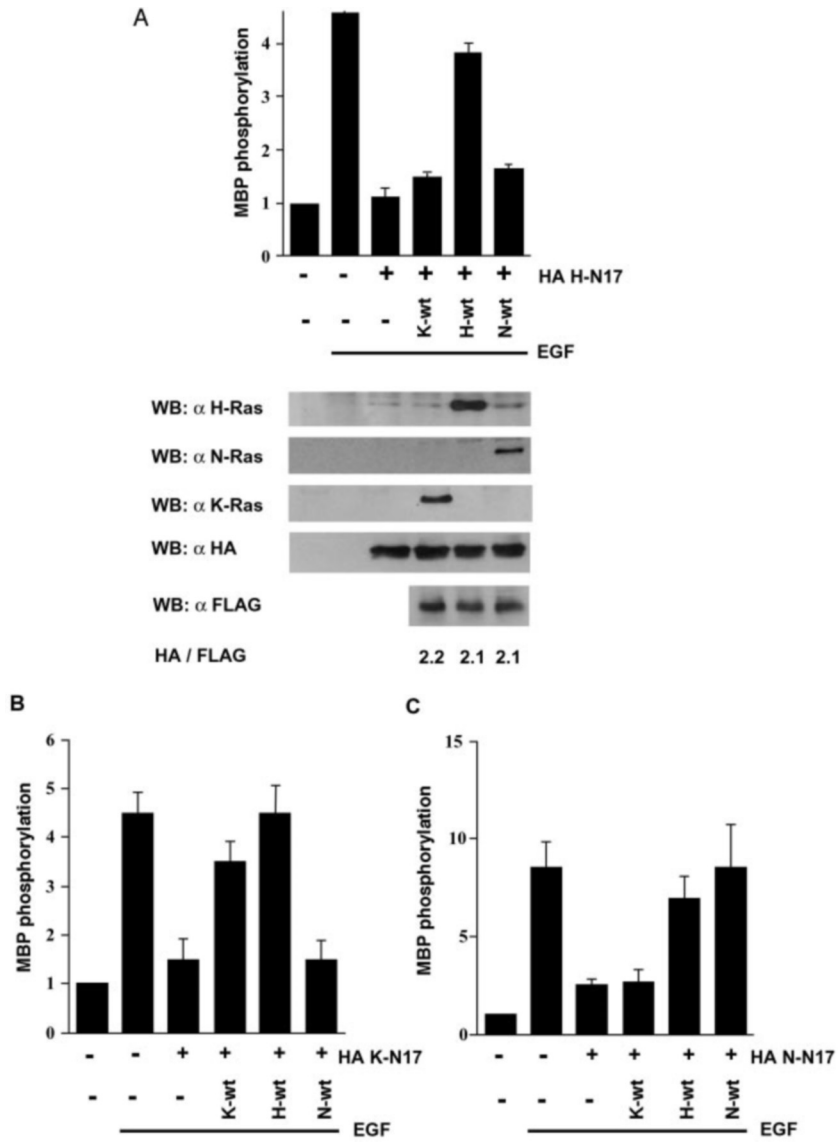

FIG. 3. **Specific rescue by Ras isoforms of the inhibition induced by H-, K-, and N-Ras N17 mutants.** *A*, rescue by H-, K-, and N-Ras of the inhibition on ERK2 activation caused by H-N17. COS-7 cells were co-transfected with AU5-ERK2 (1 μg), with vector (−), and with 250 ng of HA-tagged H-N17 (+), in addition to 500 ng, of plasmids encoding FLAG-tagged H-, K- or N-Ras wild types (wt). Upon stimulation with EGF (100 ng/ml) for 5 min, kinase assays were performed in anti-AU5 immunoprecipitates, using MBP as substrate. *Lower panels*, protein levels of H-, K-, and N-Ras as determined by immunoblotting using specific antibodies; protein levels of HA-H-N17 and of the FLAG-tagged wild-type isoforms as indicated. The panels show the ratio of the HA/FLAG signals in a representative experiment. *B*, rescue by H-, K-, and N-Ras of the inhibition on ERK2 activation caused by K-N17. *C*, rescue by H-, K-, and N-Ras of the inhibition on ERK2 activation caused by N-N17. *A–C*, data show averages ± S.E. of at least five independent experiments, relative to the MBP phosphorylation levels detected in control cells.

K-N17, and N-N17 in addition to increasing concentrations of plasmids encoding for their wild-type homologues. It was found that even at their lowest concentration, a 2-fold excess, H-, K-, and N-Ras wild types remarkably rescued the restrain exerted by their respective N17 mutants on the activation of ERK2 induced by EGF (Fig. 2). These rescues were not due to a direct activation of ERK2 by the wild-type Ras proteins, because even at their highest levels of expression, wild-type H-, K-, and N-Ras activated ERK2 very poorly (data not shown).

Next, we investigated whether the inhibitory effect exerted by a given Ras N17 mutant could be restored by the overexpression of any of the three wild-type Ras isoforms. For this purpose cells transfected with AU5-ERK2 were co-transfected with equal amounts of HA-tagged H-N17, K-N17, and N-N17 and of FLAG-tagged H-, K-, and N-Ras wild types. Then ERK2 activation was determined in anti-AU5 immunoprecipitates upon EGF stimulation. The rescue of the dominant negative constructs by overexpression of the wild-type proteins is likely to be a threshold effect. As such, small variations on the ratio of N17 and wild-type proteins may tip the balance between inhibition and activity. Therefore it was very important to control the relative levels of expression of the transfected wild types and inhibitory mutants in every case. Even though the different affinities exhibited by the FLAG and HA antibodies towards their respective epitopes precluded a precise comparison of the concentrations of each protein, the ratio between the HA and FLAG signals was extremely valuable to monitor changes in the expression of the wild-type and the inhibitory proteins relative to each other.

Interestingly, the blockade on EGF-induced ERK2 activation brought about by H-N17 could only be effectively rescued by H-Ras, whereas K-Ras and N-Ras were solely capable of slight rescues of 12 and 16%, respectively (Fig 3*A*). These differences on the rescue capabilities of each Ras isoform could not be attributed to major differences on their relative protein concentrations, because the HA/FLAG ratio was almost identical in all cases (Fig. *3A*, *lower panels*). In a similar fashion, the inhibitory effect exerted by K-N17 could be entirely overcome by H-Ras, and K-Ras was capable of a restoration up to 79%, whereas N-Ras was completely ineffective for rescuing the activation of ERK2 (Fig. 3*B*). Likewise, the inhibition caused by N-N17 was fully restored by N-Ras, and up to 78% was restored by H-Ras, but it was unaffected by the expression of K-Ras (Fig. 3*C*). These results constituted the first evidence for differential behavior of H-, K-, and N-Ras N17 mutants on their inhibitory properties.

We moved further to examine whether the membrane attachment signal could influence the ability of a Ras isoform to overcome the inhibitory effect of its respective N17 mutant. To do so, we generated an H-Ras in which cysteine 186 was de-

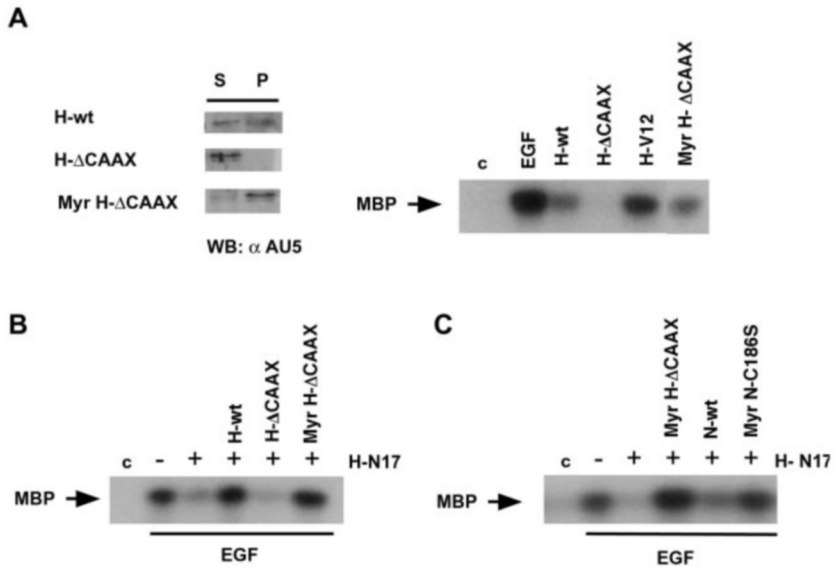

FIG. 4. **Rescue by myristoylated H-Ras of the inhibition on ERK2 activation caused by H-N17.** *A*, *left panel*, Cellular distribution of H-Ras CAA*X* mutant proteins. COS-7 cells were transfected with AU5-tagged H-Ras wild type (*wt*), H-ΔCAA*X*, and Myr-H-ΔCAA*X*, lysates were fractionated as described under "Materials and Methods," and protein expression was detected by anti-AU5 immunoblotting. *Lane S*, S100 soluble fraction; *lane P*, P100 particulate fraction. *Right panel*, ERK2 activation by H-Ras CAA*X* mutant proteins. Kinase assays from cells co-transfected with HA-ERK2 (1 μg), and the indicated Ras construct (500 ng, 100 ng for H-Ras V12), or stimulated with EGF (100 ng/ml) for 5 min, performed as previously described. *B*, rescue by Myr-H-ΔCAA*X* of the inhibition induced by H-N17. COS-7 cells were co-transfected with HA-ERK2 (1 μg), with vector (*lanes c* and −) and with 250 ng of H-N17 (*lanes* +), in addition to 500 ng of plasmids encoding for the different H-Ras proteins as indicated. Upon stimulation with EGF (100 ng/ml) for 5 min, the kinase assays were performed in anti-HA immunoprecipitates, using MBP as substrate. *C*, rescue by myristoylated N-Ras of the inhibition induced by H-N17. COS-7 cells were co-transfected with HA-ERK2 (1 μg), with vector (*lanes c* and −) and with 250 ng of H-N17 (*lanes* +), in addition to 500 ng, of plasmids encoding for the different Ras proteins as indicated. Upon stimulation with EGF (100 ng/ml) for 5 min, the kinase assays were performed in anti-HA immunoprecipitates, using MBP as substrate.

leted (H-ΔCAA*X*) and added a c-Src myristoylation signal to its N terminus (Myr-H-ΔCAA*X*), in addition to an AU5 tag to facilitate its detection. We thereby substituted a farnesylation/palmitoylation with a myristoylation/palmitoylation post-translational modification, both of which are effective membrane anchors (43). As shown in Fig. 4*A* (*left panel*), although H-ΔCAA*X* upon loosing its farnesylation site was solubilized and appeared exclusively in the cellular soluble fraction, Myr-H-ΔCAA*X* was mainly localized in the particulate fraction. As such, Myr-H-ΔCAA*X* could induce a slight activation of ERK2, comparable with that elicited by H-Ras wild type. On the other hand, H-ΔCAA*X* was incapable of activating ERK2 to any extent (Fig. 4*A*, *right panel*). When we tested the ability of these constructs to rescue the inhibition exerted by H-N17 on ERK2 activation by EGF, it was found that Myr-H-ΔCAA*X* was as competent as wild-type H-Ras for overcoming the blockade brought about by H-N17. On the other hand, H-ΔCAA*X* was completely ineffective (Fig. 4*B*). Therefore, our results indicated that myristoylated Ras proteins were as efficient as farnesylated forms for overcoming the repressing effects of Ras dominant inhibitory mutants. In light of this result, we asked whether the substitution of the farnesyl by a myristoyl post-translational modification could render other Ras isoforms competent for rescuing the inhibitory effects of H-N17. To do so, we added a c-Src myristoylation signal to the N terminus of a farnesylation-deficient N-Ras in which cysteine 186 was substituted by serine (Myr N-C186S). It was found that although wild-type N-Ras was only capable of a minor rescue on the inhibitory effect exerted by H-N17 on EGF-induced ERK2 activation, Myr N-C186S, which slightly activated ERK2 *per se* (data not shown), could significantly overcome H-N17 inhibition, although not as effectively as Myr-H-ΔCAA*X* (Fig. 4*C*).

It was of the utmost importance to determine to what extent each of the Ras dominant inhibitory mutants could inhibit the activation of three Ras isoforms. For this purpose, we examined how AU5-tagged H-N17, K-N17, and N-N17 interfered with the GDP/GTP exchange induced by EGF on HA-tagged H-, K-, and N-Ras, when transfected in COS-7 cells. These analyses were performed by the GTP-Ras pull-down assay, using Raf Ras-binding domain fused to GST (44). Surprisingly, it was found that the nucleotide exchange induced by EGF on K-Ras was completely blocked by H-N17 and K-N17 but was unaffected by N-N17 (Fig. 5*A*), even though N-N17 was expressed at levels comparable with those of H-N17 and K-N17, and the wild type and N17 relative concentrations, assessed by the HA/AU5 signals ratio, were similar in all instances (Fig. 5*A*, *lower panels*). On the other hand, the activation of H-Ras was potently suppressed by H-N17, whereas K-N17 caused a 22% inhibition, and N-N17 reduced its nucleotide exchange merely by 16% (Fig. 5*B*). In a similar fashion, GDP/GTP exchange on N-Ras induced by EGF was inhibited by H-N17 and N-N17 down to basal levels, but under the same experimental setting K-N17 had no detectable effects (Fig. 5*C*).

Based on the results described above, because N-N17 interfered with the EGF signal by specifically inhibiting the activation of N-Ras without significantly affecting K-Ras and very slightly H-Ras, it would be conceivable that in the absence of an endogenous N-Ras, the ability of N-N17 to down-regulate EGF-induced ERK2 activation would be severely impaired. Therefore, we further ascertained the specificity range of the N-N17 mutant in N-Ras-null MEFs (20). MEFs obtained from N-Ras knock-out mice (−/−) and from wild-type littermates (+/+) were transiently co-transfected with HA-ERK2 and with the AU5-tagged H-N17, K-N17, and N-N17 mutants, and ERK2 activation was determined upon stimulation with EGF. In N-Ras +/+ MEFs, all three inhibitory mutants were capable of reducing the EGF-induced ERK2 activation, with K-N17 causing the greatest repression. However, in N-Ras −/− MEFs, N-N17 was completely inefficient for down-regulating the activity of ERK2 (Fig. 5*D*), providing a further demonstration that N-N17 inhibitory effects are primarily mediated by N-Ras.

It was conceivable that the distinct inhibitory specificities

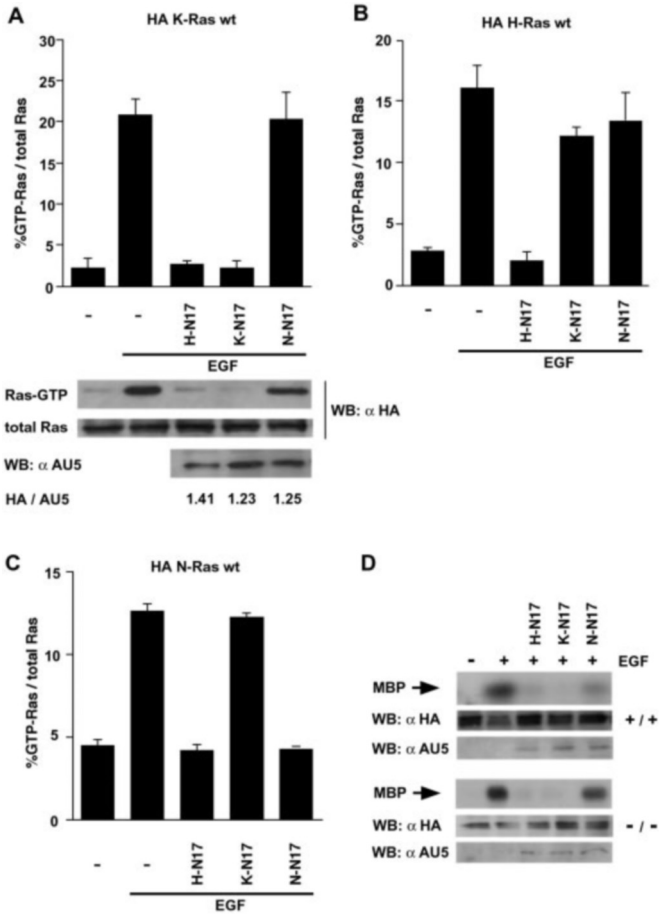

FIG. 5. **Inhibition of nucleotide exchange on Ras isoforms by H-, K-, and N-Ras N17 mutants.** *A*, inhibition of nucleotide exchange on K-Ras by H-N17, K-N17, and N-N17. Ras GTP loading was determined as described under "Materials and Methods" upon treatment with EGF (100 ng/ml) for 5 min where indicated, in COS-7 cells co-transfected with HA-K-Ras (250 ng) in the presence of vector (−) or of H-N17, K-N17, and N-N17 (250 ng of each) as shown. *Upper panel*, HA-K-Ras-GTP levels from a representative experiment, as determined by anti-HA-immunoblotting in affinity precipitates using GST-Raf Ras-binding domain as bait. *Middle panel*, total input, K-Ras levels as determined by anti-HA-immunoblotting in total lysates. *Lower panel*, protein levels of AU5-tagged H-N17, K-N17, and N-N17 as determined by anti-AU5 immunoblotting. The numbers show the ratio of the HA/AU5 signals in a representative experiment. *B*, inhibition of nucleotide exchange on H-Ras by H-N17, K-N17, and N-N17. The values were determined as described above. *C*, inhibition of nucleotide exchange on N-Ras by H-N17, K-N17, and N-N17. *A–C*, data show averages ± S.E. of at least five independent experiments. *D*, effects of Ras inhibitory mutants on EGF-induced ERK2 activation in N-Ras-null MEFs. MEFs from N-Ras-null mice (−/−) and wild-type littermates (+/+) were transiently co-transfected with HA-ERK2 (1 μg) and AU5-tagged H-N17, K-N17, and N-N17 (250 ng of each). Upon stimulation with EGF (100 ng/ml) for 5 min where indicated (+), kinase assays were performed as previously described. *Lower panels*, protein levels of HA-ERK2 and AU5-tagged inhibitory mutants as determined by immunoblotting using anti-HA and AU5-specific antibodies, respectively. *WB*, Western blot.

exhibited by H-, K-, and N-Ras dominant interfering mutants guarded some relationship with the pattern of distribution of the three Ras isoforms in different plasma membrane microdomains. The compartmentalization of H-Ras and K-Ras is well documented, whereas H-Ras is mainly found in lipid rafts, both caveolar and noncaveolar, K-Ras is present in the bulk, disordered membrane (26, 27, 31, 45). However, a detailed study on N-Ras cellular distribution is still missing. As a first approach to ascertain the nature of the plasma membrane microlocations where N-Ras was positioned, we carried out a Triton X-100

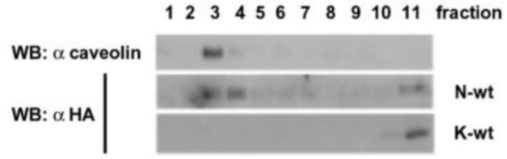

FIG. 6. **Association of N-Ras to lipid rafts.** COS-7 cells were transfected with HA-tagged K-Ras and N-Ras. Cells solubilized in 0.250% Triton X-100 were partitioned in a sucrose gradient as described under "Materials and Methods." The presence of the Ras isoforms in the different fractions was analyzed by anti-HA immunoblotting. Anti-caveolin-1 immunoblotting identifies the lipid raft fractions. *WB*, Western blot; *wt*, wild type.

solubility test to assay for lipid raft association, because lipid rafts are insoluble in this detergent (26). As such, COS-7 cells were transfected with HA-tagged K-Ras and N-Ras, and their solubility in 0.25% Triton X-100 was determined. As shown in Fig. 6, after resolution in a sucrose gradient, 75–80% of N-Ras was detected in the same fractions as caveolin-1, a marker for lipid rafts. On the other hand, K-Ras was completely solubilized in 0.25% Triton and appeared in the denser fractions, thereby demonstrating a prominent association of N-Ras to lipid rafts.

To undertake in further detail the ultrastructural analysis of N-Ras distribution, MDCK cells were transfected with constructs encoding green fluorescent protein (GFP) with N-Ras or N-Ras hypervariable region (amino acids 163–189) fused to its C terminus and examined using immunogold electron microscopy with antibodies that recognize the GFP tag. To avoid artifactual localizations caused by overexpression, low levels of expression were chosen, that is, cultures in which Western blotting showed a clear anti-GFP signal but in which an anti-N-Ras signal did not reach a 2-fold increase over the endogenous N-Ras levels (data not shown). GFP-N-Ras was clearly localized in electron-dense areas on the plasma membrane, both at the cell body and tapered cellular processes (Fig. 7, *A* and *B*). However, no specific labeling was detectable in caveolae (Fig. 7*A*, *arrow*), whereas in cells transfected with GFP-H-Ras, H-Ras was clearly visible in caveolar membranes (Fig. 7*C*, *arrow*). The comparative analysis of the subcellular distribution of GFP-N-Ras and GFP-H-Ras showed that both fusion proteins were detectable on electron-dense areas of the plasma membrane. Interesting, a high density of gold particles was found on the membrane domains that formed the boundary of filopodia (Fig. 7, *D–F*, *arrows*). Like GFP-N-Ras, some scattered gold particles of GFP-H-Ras decorated the cytosol in areas rich in intermediate filaments, but in either case, no labeling was observed on rough endoplasmic reticulum membranes (Fig. 7, *D* and *G*). Within the cytoplasm, gold particles of GFP-N-Ras immunoreactivity were mainly distributed on the mitochondria (Fig. 7*H*) and particularly in areas enriched in intermediate filament bundles (Fig. 7*G*, *if*). No differences in localization were detected when using GFP-N-Ras hypervariable region when compared with GFP-N-Ras (data not shown).

In light of our data, we proceeded to use H-, K-, and N-Ras inhibitory mutants as tools to investigate how the signals induced by various stimuli and GEFs, resulting in the activation of ERK2, were affected by the differential blockade on the total Ras output. As such, NIH3T3 cells were transiently co-transfected with HA-ERK2 and with the H-N17, K-N17, and N-N17 mutants and stimulated with PDGF or with LPA. As shown in Fig. 8*A*, the activation of ERK2 by PDGF was markedly down-regulated by H-N17 and K-N17 but not by N-N17 (Fig. 8*A*). On the other hand, all three inhibitory mutants could repress the LPA-induced activation of ERK2, of which K-N17 caused the largest suppression.

In the same fashion, we finally investigated the effects of the

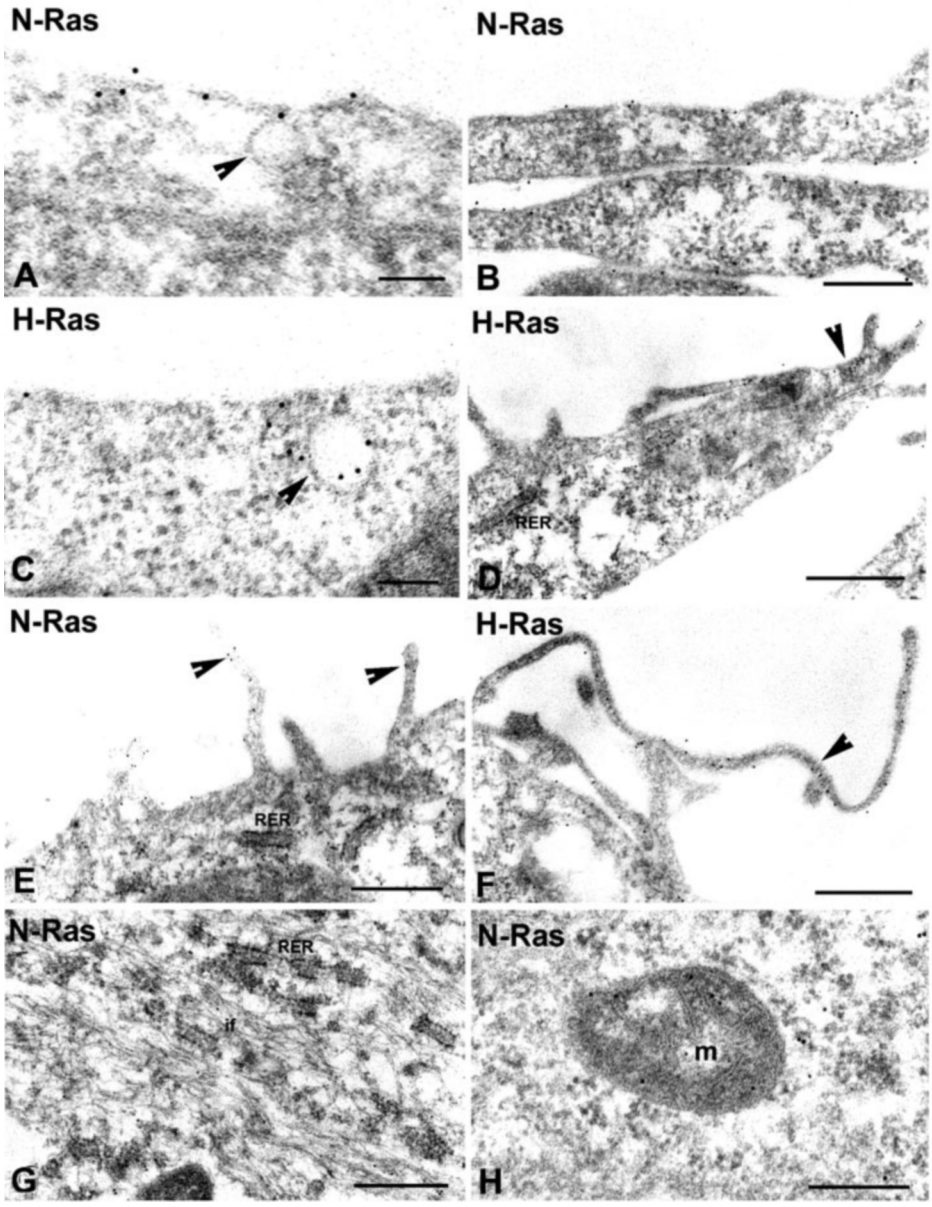

FIG. 7. **Immunogold electron microscopy localization of GFP-N-Ras in MDCK cells using antibodies against GFP and a secondary antibody conjugated with 10 nm gold particles.** Specific labeling of GFP-N-Ras is observed on electron-dense areas of the plasma membrane (*A* and *B*). Caveolae (*arrowhead* in *A*) appear free of labeling. Conversely, GFP-H-Ras was clearly present in caveola (*arrowhead* in *C*). Note in *D* the high concentration of H-Ras gold labeling on the tip of a cellular process (*arrowhead* in *D*). Both GFP-N-Ras and GFP-H-Ras were clearly distributed on the plasma membrane with a higher concentration detected on the membrane of filopodia (*E* and *F*). In the cytoplasm, a few gold particles of N-Ras immunoreactivity decorated the cytosol, in areas occupied by intermediate filaments (*G*, *if*). Gold particles also decorated the mitochondrial matrix (*M*). There was a negligible labeling on the rough endoplasmic reticulum (*RER*) (*D*, *E*, and *G*). *Scale bars*, 100 nM in *A* and *C*; 300 nM for the rest.

Ras inhibitory mutants in the stimulation of ERK2 by Ras-activating GEFs. To do so, COS-7 cells were co-transfected with HA-ERK2 and the H-N17, K-N17, and N-N17 mutants, in addition to the different GEFs to be tested. Activation of ERK2 by SOS1 was equally blocked by the three inhibitory mutants (Fig. 8*B*). ERK2 activation by Ras-GRF1 was only repressed by H-N17 but was unaffected by K-N17 and N-N17. A similar situation was observed with Ras-GRF2, but in this case, K-N17 and N-N17 were capable of inducing a noticeable inhibition on ERK2 activation. Interestingly, the stimulatory effects of the Ras exchange factor Cal-DAG I on the activation of ERK2 were completely unaffected by H-N17, K-N17, and N-N17. Conversely, Cal-DAG II behaved similarly to SOS1; its ability to activate ERK2 was equally blocked by the three Ras inhibitory mutants. On the other hand, ERK2 activation by Cal-DAG III was markedly inhibited by H-N17 and to a lesser extent by K-N17 and N-N17. Overall, our results clearly indicated that H-, K-, and N-Ras N17 mutants had distinct inhibitory effects over most of the Ras-activating GEFs described thus far.

To enable us a better interpretation of these results, we ascertained the ability of the different GEFs to stimulate guanine nucleotide exchange on the three Ras isoforms. In full agreement with previous results (15, 29), we found that SOS induced exchange on the three Ras isoforms, and Ras-GRF1 was active solely over H-Ras (data not show). On the other hand, Ras-GRF2 induced a potent GDP/GTP exchange on H-Ras and to a lesser extent on N-Ras and K-Ras (Fig. 8*C*). In the case of the CAL-DAG family, CAL-DAG II could stimulate a remarkable nucleotide exchange on the three isoforms. On the other hand, CAL-DAG III catalyzed GDP/GTP replacement to a different degree in the three Ras proteins, being most active on H-Ras and least over K-Ras. By contrast, CAL-DAG I was incapable of inducing exchange on any of the three Ras isoforms.

DISCUSSION

In this study we have investigated the inhibitory specificities that H-Ras, K-Ras4B, and N-Ras N17 dominant inhibitory mutants exhibit toward the activation of the wild-type Ras isoforms. We have found that H-N17, K-N17, and N-N17 display remarkable differences in their ability to inhibit the activation of ERK2 and the nucleotide exchange on H-Ras, K-Ras4B, and N-Ras, induced by EGF. A straightforward explanation for these variations would be that the three Ras dominant inhibitory mutants posses different affinities toward

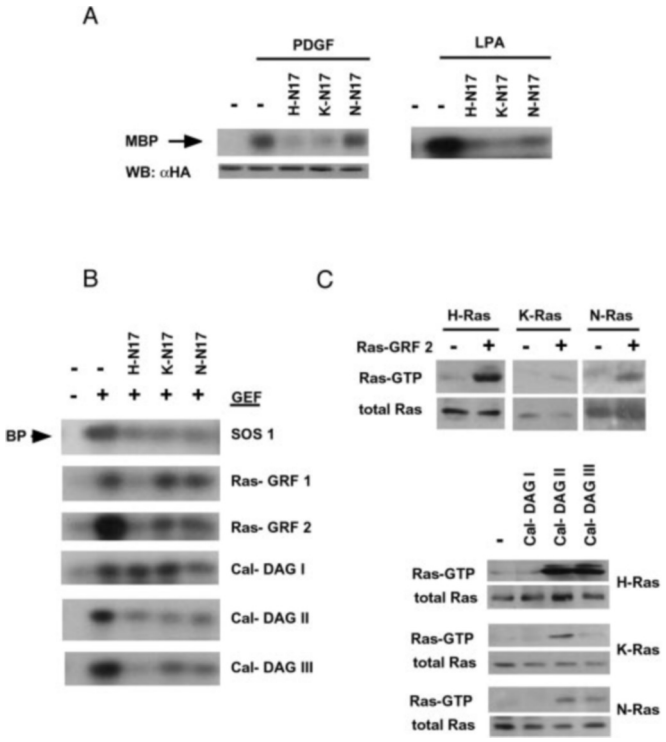

FIG. 8. **Effects of Ras inhibitory mutants on ERK2 activation induced by mitogenic stimuli and Ras-activating GEFs.** *A*, effects of Ras inhibitory mutants on the activation of ERK2 induced by mitogens. NIH3T3 cells were transiently transfected with HA-ERK2 (1 μg) and with AU5-tagged H-N17, K-N17, and N-N17 (250 ng of each). Upon stimulation with PDGF (10 ng/ml) or with LPA (10 μM) for 5 min where indicated, kinase assays were performed as previously described. *Lower panel*, protein levels of HA-ERK2 as determined by immunoblotting using an HA-specific antibody. *B*, effects of Ras inhibitory mutants on the activation of ERK2 induced by Ras-activating GEFs. COS-7 cells were transiently transfected with HA-ERK2 (1 μg) and with AU5-tagged H-N17, K-N17, and N-N17 (250 ng of each), in addition to the different GEFs (0.5 μg), where indicated (+). The kinase assays were performed as previously described. *C*, GDP/GTP exchange induced on H-, K-, and N-Ras by Ras-activating GEFs. Ras GTP loading was determined as described under "Materials and Methods," in COS7 cells transfected with the indicated GEFs (0.5 μg) and the HA-tagged Ras isoforms (1 μg) as shown. *WB*, Western blot.

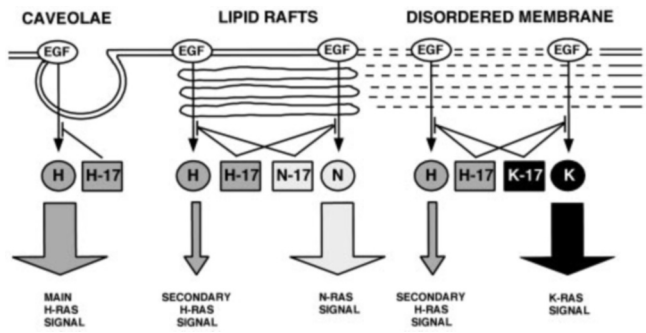

FIG. 9. **Model for Ras dominant inhibitory mutants effects on different plasma membrane microlocations.** H-Ras would be present in caveolae, in noncaveolar lipid rafts where it would co-localize with N-Ras, and in disordered plasma membrane in addition to K-Ras. As such, H-N17 would be present in all of these microlocations. K-N17 presence would be restricted to bulk membrane, and N-N17 would be solely found in lipid rafts. Therefore, H-N17 would block the activation of H-Ras main signal in caveolae, the activation of an H-Ras secondary signal and of N-Ras in rafts, and the activation of another H-Ras secondary signal and of K-Ras in bulk membrane. On the other hand, K-N17 inhibitory effect would be restricted to the bulk membrane, where it would block the secondary H-Ras-mediated component and the K-Ras signal. Likewise, N-N17 would inhibit the activation of its wild-type counterpart and the activation of the H-Ras component that occurs in lipid rafts.

the GEFs activated by EGF. Of all the Ras-activating GEFs described up to date, only SOS 1–2 and Ras-GRF2 are ubiquitously expressed (46, 47). In the experimental model utilized in this study, COS-7 cells, we have not detected expression of Ras-GRF2.[2] Furthermore, Ras-GRF2 is essentially activated by G-protein-coupled receptors, not by the tyrosine kinase type, like the EGF receptor (47). Therefore, it is predictable that the EGF-induced events described herein are mainly mediated by SOS, notwithstanding the participation of other, as yet unidentified GEFs.

To the best of our knowledge, a comparative study on the binding affinities that SOS exhibits toward H-, K-, and N-Ras has not been reported. However, major differences are not to be expected. First, regarding the structure, the resolution of the SOS-Ras complex has revealed that the residues in Ras that determine the binding to SOS are highly conserved among H-, K-, and N-Ras (48). Second, any existing differences on the binding affinities of SOS and the three Ras isoforms would be reflected by the efficiency with which SOS stimulates nucleotide exchange in H-, K-, and N-Ras *in vitro*. As such, it is known that SOS induces GDP/GTP exchange on the three isoforms in the hierarchy H-Ras > N-Ras > K-Ras (29). However, the recorded variations in the nucleotide replacement induced by SOS on the different Ras isoforms are small.[3] This also occurs for other GEFs such as Ras-GRF1. In this case, differences on its exchange potential do not even reach 2-fold between any two Ras isoforms (49). In light of these considerations, it is unlikely that distinct GEF binding affinities can account for the dramatic differences that H-, K-, and N-Ras N17 mutants display in their capacity to inhibit Ras functions in EGF-induced episodes.

An alternative explanation could be found in the recently reported compartmentalization of Ras proteins in distinct plasma membrane domains (25). It has been shown that H-Ras is distributed approximately equally in caveolar and noncaveolar lipid rafts and bulk plasma membrane. On the other hand, K-Ras is localized predominantly in nonraft bulk membrane (26, 31, 45). A recent report also localizes K-Ras in caveolae (27). However, this last conclusion is reached by co-localization with caveolin using confocal microscopy, as opposed to the previous studies that utilize electron microscopy. It is debatable whether confocal microscopy can offer the necessary resolution to discriminate accurately between caveolae and contiguous bulk membrane. Herein, we present for the first time the ultrastructural localization of N-Ras. We have found that N-Ras is mainly present in lipid rafts, in agreement with other investigators.[3] However, we have not detected N-Ras in caveolae, in contradiction to a previous report using confocal microscopy (27). Our results indicate that N-Ras also co-localizes with H-Ras in the membrane and tips of cellular prolongations and filopodia. We have also detected N-Ras in mitochondria, in consonance with previous reports (50), something that may be directly related to the steady-state antiapoptotic signal generated by N-Ras (51). Interestingly, some N-Ras co-localizes in the cytoplasm with intermediate filaments, a connection unprecedented thus far. It is likely that the N-Ras associated with mitochondria and intermediate filaments accounts for the portion of N-Ras, about 20%, detected in the last fractions of the sucrose gradients.

Basing ourselves in the above mentioned distribution of the three Ras isoforms in distinct plasma membrane microdo-

[2] I. Arozarena and P. Crespo, unpublished results.

[3] J. F. Hancock, personal communication.

mains, we propose the model depicted in Fig. 9 to explain our results on the inhibitory properties of H-, K-, and N-Ras N17 dominant inhibitory mutants. As discussed before, H-Ras is present: in caveolae, in noncaveolar lipid rafts where it co-localizes with N-Ras, and in the disordered, bulk plasma membrane where it co-exists with K-Ras. Therefore, it would be conceivable to find H-N17 in all these compartments. On the other hand, the presence of K-N17 would be restricted to bulk membrane, and N-N17 would be solely found in lipid rafts. Although H-Ras is equally present in the three membrane microdomains, there is evidence suggesting that H-Ras activation takes place primarily in caveolae (26, 45, 52–54). Even though the main H-Ras signal may originate in caveolae, the presence of H-Ras in rafts and bulk membrane makes it conceivable that secondary, less intense H-Ras-mediated signals can also arise in these locations, where the respective N-Ras and K-Ras activation takes place as well.

As such, H-N17 would block the activation of H-Ras main signal in caveolae, the activation of an H-Ras secondary signal and of N-Ras in rafts, and the activation of another H-Ras secondary signal and of K-Ras in bulk membrane. This agrees with our data demonstrating that inhibition by H-N17 is greatly rescued by the overexpression of H-Ras wild type, which restitutes the H-Ras signal in all locations. Conversely, H-N17 inhibition is only slightly rescued by K-Ras (12%), which partially restores the EGF-induced signal generated in bulk membrane, and by N-Ras (16%), which can only re-establish the signal in lipid rafts. On the other hand, K-N17 completely inhibits the activation of K-Ras and partially blocks H-Ras activation (22%), because it can only interfere with the H-Ras-mediated component that originates in bulk membrane. Because K-N17 is not present in lipid rafts, it does not affect N-Ras activation whatsoever. Accordingly, because the K-N17 inhibitory effect is restricted to the bulk membrane, it can be rescued by the overexpression of the Ras isoforms that are located therein, H-Ras and K-Ras itself, as our data demonstrate. Likewise, N-N17 completely inhibits the activation of its wild-type counterpart and blocks the activation of the H-Ras component that operates in lipid rafts (16%). In agreement, we show that the overexpression of wild-type H-Ras and of N-Ras counteracts N-N17 inhibitory effect, which takes place solely in lipid rafts. Because N-N17 is not present in bulk membrane, it does not affect K-Ras activation. Overall, this model reconciles our results about the inhibitory properties of Ras dominant interfering mutants, with the present knowledge on the compartmentalization of Ras isoforms. These data, obtained in COS-7 cells, are strongly validated by our experiments in N-Ras-null fibroblast. In this cellular setting, we demonstrate that the absence of endogenous N-Ras severely precludes N-N17 inhibitory effects, without affecting those of H-N17 and K-N17.

Our results also indicate that the substitution of the farnesyl anchor for a myristoylation signal in H-Ras does not affect the ability of the resulting myristoylated/palmitoylated H-Ras to rescue the inhibitory effect elicited by H-N17. Interestingly, switching the farnesyl anchor for a myristoylation signal also potentiates the competence of N-Ras for counteracting the inhibition exerted by H-Ras N17. A likely explanation for these phenomena is provided by recent reports indicating that myristoylated H-Ras is distributed through the plasma membrane in a similar way to wild-type H-Ras (29). Thus, it is conceivable that myristoylation would alter N-Ras location within the membrane and augment its concentration at sites where it co-localizes with H-Ras, thereby enabling it to counterbalance H-N17 inhibitory effects.

Having established the specificity range for H-, K-, and N-Ras dominant inhibitory mutants, we have used them as tools to investigate the relative contribution of their wild-type counterparts to the signals generated by a series of mitogenic stimuli driven through different types of membrane receptors. The use of these mutants would also be extremely helpful for identifying the plasma membrane compartment in which these signals are generated. We have shown that the activation of ERK2 by EGF is inhibited by the three Ras inhibitory mutants, but to different extent: almost total inhibition by H-N17, 88% repression by K-N17, and 55% inhibition by N-N17. Because the inhibition brought about by H-N17 results from blocking the signals generated in caveolae, rafts, and bulk membrane, whereas the repression by K-N17 is solely due to the inhibition of the bulk membrane-originated signal, this would suggest that K-Ras is the main Ras isoform conveying the EGF signal to the ERKs cascade. A similar situation is observed in the case of PDGF, which is equally inhibited by H-N17 and K-N17 but is largely unaffected by N-N17, in consonance with previous results indicating that PDGF signals are not efficiently conveyed by N-Ras (55). The prevalence of the bulk membrane K-Ras component is also remarkable in the case of the activation of ERK2 stimulated by LPA, which is repressed most potently by K-N17.

In a similar fashion, we have utilized H-, K-, and N-Ras dominant inhibitory mutants to give us an insight into the sites of action and isoform specificity displayed *in vivo* by most Ras-activating GEFs described thus far. As such, our data show that the activation of ERK2 by Ras-GRF1 is inhibited by H-N17 but is completely unaffected by K-N17 and N-N17. This result indicates that Ras-GRF1 can only signal through H-Ras, in perfect agreement with previous results showing that, *in vivo*, Ras-GRF1 induces GDP/GTP exchange in H-Ras but not in K-Ras nor in N-Ras (15). A similar situation is observed for Ras-GRF2; only in this case, K-N17 and N-N17 can slightly diminish the signal elicited by this GEF. These results could be interpreted as Ras-GRF1 inducing the activation of H-Ras solely in caveolae, whereas Ras-GRF2 would be capable of activating, to a lesser extent, the lipid rafts and bulk membrane components of the total Ras signal. Indeed, we demonstrate that Ras-GRF2 is capable of stimulating GDP/GTP exchange on N-Ras and on K-Ras, although at lower levels than on H-Ras.

In the case of CAL-DAG III, its potential to activate ERK2 is remarkably inhibited by H-N17, and to a lesser extent by K-N17 and N-N17, thereby pointing to the H-Ras/caveolar component as the main route used by this GEF for activating ERK2. Also in the case of this GEF, the effects exhibited by the Ras inhibitory mutants on its function match closely its affinity for the three Ras isoforms as demonstrated by *in vivo* exchange assays. As such, we show that CAL-DAG III is primarily active on H-Ras and exhibits weaker exchange activities on N-Ras and K-Ras.

Particularly intriguing situations are those detected for SOS1 and CAL-DAG II, in these two cases, the three N17 mutants suppress ERK2 activation with similar efficiency. This was unexpected because, in light of our model, if the signals generated in caveolae, rafts, and bulk membrane were equal, H-N17 would be expected to exert a greater inhibition than the other two N17 mutants. Although we do not have a precise answer for this phenomenon, one possible explanation could be that the expression levels of these GEFs are high enough as to overcome the inhibitory effects of the N17 mutants in all locations. A second possibility would be that the Ras dominant inhibitory mutants completely suppress the activation of ERK2 brought about by the total Ras component and the residual activation being due to the stimulation by SOS or

CAL-DAG II of an ERK-activating pathway mediated by another GTPase. Indeed, both SOS and CAL-DAG II can stimulate nucleotide exchange on M-Ras, and CAL-DAG II is also active over TC21 (56). A similar situation may be occurring in the case of CAL-DAG I. We and others (16) have demonstrated that this GEF cannot induce nucleotide exchange on any of the three Ras isoforms. Nevertheless, our results clearly show that CAL-DAG I can induce a potent ERK2 activation that is insensible to inhibition by H-N17, K-N17, and N-N17. Because CAL-DAG I is an effective GEF for Rap-1 (16), it is likely that CAL-DAG I may be activating ERK2 through a Rap > B-Raf > MEK pathway, independently of Ras.

In summary, our data clearly indicate that, regardless of the fact that the three Ras isoforms share most known GEFs, the inhibitory spectra of H-, K-, and N-Ras N17 dominant inhibitory mutants are remarkably different. Furthermore, we show that the inhibitory specificities displayed by these mutants can be reasonably explained in view of the recent findings on the compartmentalization of Ras proteins in distinct membrane microdomains. This situation may find a precedent in the case of Rho family GTPases. It is now well known that most Dbl family GEFs are active on Rho, Rac, and Cdc42 (35). However, the widespread use of Rho, Rac, and Cdc42 dominant inhibitory mutants has yielded remarkably specific inhibitions. In light of our findings, it is likely that this specificity is also based to a great extent on the microlocalization of each Rho family member. As is the case for the Rho GTPases dominant inhibitory mutants, our results provide the basis for H-, K-, and N-Ras dominant inhibitory mutants to become useful tools for further investigating Ras functions and the differences among H-Ras, K-Ras, and N-Ras.

Acknowledgments—We thank Drs. M. Matsuda, J. C. Stone, and M. F. Moran for providing us with reagents, Dr. J. F. Hancock for sharing unpublished information, Drs. Alfred Wittinghofer and Javier León for helpful discussions, and Salvador Aznar for technical assistance.

REFERENCES

1. Malumbres, M., and Pellicer, A. (1998) *Fronts. Biosci.* **3,** 887–912
2. Crespo, P., and Leon, J. (2000) *Cell. Mol. Life Sci.* **57,** 1613–1636
3. Lowy, D. R., and Willumsem, B. M. (1993) *Annu. Rev. Biochem.* **62,** 851–891
4. Willumsem, B. M., Christensen, A., Hubbert, N. L., Papageorge, A. G., and Lowy, D. R. (1984) *Nature* **310,** 583–586
5. Hancock, J. F., Magee, A. I., Childs, J. E., and Marshall, C. J. (1989) *Cell* **57,** 1167–1177
6. Hancock, J. F., Paterson, H., and Marshall, C. J. (1990) *Cell* **63,** 133–139
7. Hancock, J. F., Cadwallader, K., Paterson, H., and Marshall, C. J. (1991) *EMBO J.* **10,** 4033–4039
8. Leon, J., Guerrero, I., and Pellicer, A. (1987) *Mol. Cell. Biol.* **7,** 1535–1540
9. Fiorucci, G., and Hall, A. (1986) *Biochym. Biophys. Acta* **950,** 81–83
10. Muller, R., Slamon, D. J., Adamson, E. J., Tremblay, J. M., Muller, D., Cline, M. J., and Verma, I. M. (1983) *Mol. Cell. Biol.* **3,** 1062–1069
11. Bos, J. L. (1989) *Cancer Res.* **49,** 4682–4689
12. Rodenhuis, S. (1992) *Semin. Cancer Biol.* **3,** 241–247
13. Maher, J., Baker, D. A., Manning, M., Dibb, N. J., and Roberts, I. A. G. (1995) *Oncogene* **11,** 1639–1647
14. Bollag, G., and McCormick, F. (1991) *Nature* **351,** 576–579
15. Jones, M. K., and Jackson, J. H. (1998) *J. Biol. Chem.* **273,** 1782–1787
16. Clyde-Smith, J., Silins, G., Gartside, M., Grimmond, S., Etheridge, M., Apolloni, A., Hayward, N., and Hancock, J. F. (2000) *J. Biol. Chem.* **275,** 32260–32267
17. Yan, J., Roy, S., Apolloni, A., Lane, A., and Hancock, J. F. (1998) *J. Biol. Chem.* **273,** 24052–24056
18. Voice, J. K., Klemke, R. I., Le, A., and Jackson, J. H. (1999) *J. Biol. Chem.* **274,** 17164–17170
19. Walsh, A. M., and Bar-Sagi, D. (2001) *J. Biol. Chem.* **276,** 15609–15615
20. Umanoff, H., Edelman, W., Pellicer, A., and Kucherlapati, R. (1995) *Proc. Natl. Acad. Sci. U. S. A.* **92,** 1709–1713
21. Ise, K., Nakamura, K., Nakao, K., Shimuzu, S., Harada, H., Ichise, T., Miyoshi, J., Gondo, Y., Ishikawa, T., Aiba, A., and Katsuki, M. (2000) *Oncogene* **19,** 2951–2956
22. Esteban, L. M., Vicario-Arbejon, C., Fernandez-Salguero, P., Fernandez-Melarde, A., Swaminathan, N., Yienger, K., Lopez, E., McKay, R., Ward, J. M., Pellicer, A., and Santos, E. (2001) *Mol. Cel. Biol.* **21,** 1444–1452
23. Johnson, L., Greenbaum, D., Cichowski, K., Mercer, K., Murphy, E., Schmitt, E., Bronson, M. T., Umanoff, H., Edelmann, W., Kucherlapati, R., and Jacks, T. (1997) *Genes Dev.* **11,** 2468–2481
24. Koera, K., Nakamura, K., Nakao, K., Miyoshi, J., Toyoshima, K., Hatta, T., Otani, H., Aiba, A., and Katsuki, M. (1997) *Oncogene* **15,** 1151–1159
25. Prior, I. A., and Hancock, J. F. (2001) *J. Cell Sci.* **114,** 1603–1608
26. Prior, I. A., Harding, A., Yan, J., Sluimer, J., Parton, R. G., and Hancock, J. F. (2001) *Nat. Cell Biol.* **3,** 368–375
27. Kranenburg, O., Verlaan, I., and Moolenar, W. H. (2001) *Curr. Biol.* **11,** 1880–1884
28. Welman, A., and Burger, M. M. (2000) *Oncogene* **19,** 4582–4591
29. Jaumot, M., Yan, J., Clyde-Smith, J., Sluimer, J., and Hancock, J. F. (2002) *J. Biol. Chem.* **277,** 272–278
30. Choy, E., Chiu, V. K., Silletti, J., Feoktistov, M., Morimoto, T., Michaelson, D., Ivanov, I. E., and Philips, M. R. (1999) *Cell* **98,** 69–80
31. Apolloni, A., Prior, I. A., Lindsay, M., Parton, R. G., and Hancock, J. F. (2000) *Mol. Cell. Biol.* **20,** 2475–2487
32. Feig, L. A. (1999) *Nat. Cell Biol.* **1,** 25–27
33. Sigal, I., Gibbs, J. B., D'Alonzo, J. S., Temeles, G. H., Wolanski, B. S., Socher, S. H., and Scolnick, E. M. (1986) *Proc. Natl. Acad. Sci. U. S. A.* **83,** 952–956
34. Feig, L. A., and Cooper, G. M. (1988) *Mol. Cell. Biol.* **8,** 3235–3243
35. Whitehead, I. P., Campbell, S., Rossmann, K. L., and Der, C. J. (1997) *Biochim. Biophys. Acta* **1332,** F1–F23
36. Coso, O. A., Chiariello, M., Yu, J. C., Teramoto, H., Crespo, P., Xu, N., Miki, T., and Gutkind, J. S. (1995) *Cell* **81,** 1137–1146
37. Arozarena, I., Aaronson, D. S., Matallanas, D., Sanz, V., Ajenjo, N., Tenbaum, S., Teramoto, H., Ighishi, T., Zabala, J. C., Gutkind, J. S., and Crespo, P. (2000) *J. Biol. Chem.* **275,** 26441–26448
38. Ajenjo, N., Aaronson, D. S., Ceballos, E., Richard, C., León, J., and Crespo, P. (2000) *J. Biol. Chem.* **275,** 7189–7197
39. Arozarena, I., Matallanas, D., and Crespo, P. (2001) *J. Biol. Chem.* **276,** 21878–21884
40. Kamata, T., and Feramisco, J. R. (1984) *Nature* **310,** 147–150
41. Crespo, P., Xu, N., Simonds, W. F., and Gutkind, J. S. (1994) *Nature* **369,** 418–420
42. Stacey, D. W., Feig, L. A., and Gibbs, J. A. (1991) *Mol. Cell. Biol.* **11,** 4053–4064
43. Cadwallader, K. A., Paterson, H., MacDonald, S. G., and Hancock, J. F. (1994) *Mol. Cell. Biol.* **14,** 4722–4730
44. Taylor, S. J., and Shalloway, D. (1996) *Curr. Biol.* **6,** 1621–1627
45. Roy, S., Luetterforst, R., Harding, A., Apolloni, A., Etheridge, M., Stang, E., Rolls, B., Hancock, J. F., and Parton, R. G. (1999) *Nat. Cell Biol.* **1,** 98–105
46. Botwell, D., Fu, P., Simon, M., and Senior, P. (1992) *Proc. Natl. Acad. Sci. U. S. A.* **89,** 6511–6515
47. Fan, N. P., Fan, W., Wang, Z., Zhang, L., Chen, H., and Moran, F. M. (1997) *Mol. Cell. Biol.* **17,** 1396–1406
48. Boriack-Sjodin, P. A., Margarit, S. M., Bar-Sagi, D., and Kuriyan, J. (1998) *Nature* **394,** 337–343
49. Lenzen, C., Cool, R. H., Prinz, H., Kuhlman, J., and Wittinghofer, A. (1998) *Biochemistry* **37,** 7420–7430
50. Rebollo, A., Perez-Sala, D., and Martinez-Arias, C. (1999) *Oncogene* **18,** 4930–4939
51. Wolfman, J. C., and Wolfman, A. (2000) *J. Biol. Chem.* **275,** 19315–19323
52. Mineo, C., James, G. L., Smart, E. J., and Anderson, R. G. W. (1996) *J. Biol. Chem.* **271,** 11930–11935
53. Liu, P., Ying, Y., Ko, Y., and Anderson, R. G. W. (1996) *J. Biol. Chem.* **271,** 10299–10303
54. Liu, P., Ying, Y., and Anderson, R. G. W. (1997) *Proc. Natl. Acad. Sci. U. S. A.* **94,** 13666–13670
55. Wakelam, M. J., Davies, S. A., Houslay, M. D., McKay, I., Marshall, C. J., and Hall, A. (1986) *Nature* **323,** 173–176
56. Ohba, Y., Mochizuki, N., Yamashita, S., Chan, A. M., Schrader, J. W., Hattori, S., Nagashima, K., and Matsuda, M. (2000) *J. Biol. Chem.* **275,** 20020–20026